

Concentration Hysteresis in the Oxidation of Methane over Pt/ γ -Al₂O₃: X-ray Absorption Spectroscopy and Kinetic Study

Ilya Yu. Pakharukov,^{†,‡} Alexander Yu. Stakheev,[§] Irina E. Beck,[†] Yan V. Zubavichus,^{||} Vadim Yu. Murzin,^{||,⊥} Valentin N. Parmon,^{†,‡} and Valerii I. Bukhtiyarov*,^{†,‡,#}

[†]Boreskov Institute of Catalysis SB RAS, Lavrentieva avenue 5, 630090 Novosibirsk, Russia

[‡]Novosibirsk State University, Pirogova street 2, 630090 Novosibirsk, Russia

[§]Zelinskii Institute of Organic Chemistry RAS, Leninsky avenue 47, 119991 Moscow, Russia

^{||}National Research Center “Kurchatov Institute”, Kurchatov square 1, 123182 Moscow, Russia

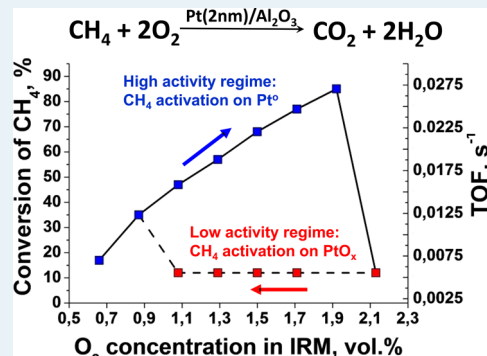
[⊥]Topchiev Institute of Petrochemical Synthesis RAS, Leninsky avenue 29, 119991 Moscow, Russia

[#]Research and Educational Center for Energy Efficient Catalysis, Novosibirsk State University, Pirogova street 2, 630090 Novosibirsk, Russia

S Supporting Information

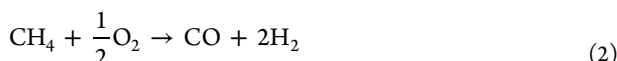
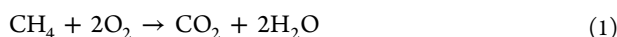
ABSTRACT: It is found that CH₄ oxidation over Pt/Al₂O₃ catalyst at 330–460 °C can stably proceed via two distinctly different regimes at identical feed gas composition: “low activity regime” and “high activity regime”. Switching between the regimes depends on the O₂ concentration and the direction of its change. For the reaction mixture with constant methane concentration of 1%, the incremental decrease in O₂ concentration from 2.5% (O₂/CH₄ ~ 2.5, lean conditions) to ~1% (O₂/CH₄ ~ 1, stoichiometric or rich conditions) results in the catalyst activation and its switching to the high activity regime. The catalyst remains active upon further incremental increase in O₂ concentration until reaching O₂/CH₄ ~ 2, when switching to low activity regime takes place. Such responses of the catalyst activity to the changes in the feed gas composition result in the appearance of the pronounced concentration hysteresis. The evident correlation between in situ X-ray absorption spectroscopy and catalytic data strongly suggests that the switching of the catalyst between low activity regime and high activity regime, which causes the concentration hysteresis, stems from the change in the electronic state of Pt particles. According to in situ XANES data, the electron density on the Pt particles decreases in the low activity regime, as evidenced by an increased Pt-L₃ white line intensity. In contrast, switching the catalyst to high activity regime is accompanied by a decrease in the white line intensity, indicating the electron density increase. In turn, the changes in the Pt electronic state are attributable to changes in the O/Pt surface ratio or formation/decomposition of a two-dimensional layer of surface Pt oxide triggered by variation of oxygen concentration in the reaction mixture. The addition of highly reactive CO or H₂ to the reaction mixture shifts the hysteresis loop toward higher oxygen concentration as a result of consuming oxygen in H₂ or CO oxidation, which decreases the effective oxygen concentration. In contrast to this, the increase in the methane concentration widens the hysteresis window, presumably because of the different stoichiometry of CH₄ oxidation upon catalyst activation (when partial CH₄ oxidation prevails) and deactivation (when total oxidation of CH₄ predominates).

KEYWORDS: methane, catalytic oxidation, concentration hysteresis, X-ray absorption spectroscopy, platinum, alumina



1. INTRODUCTION

The practically important reactions of total and partial oxidation of methane (eqs 1 and 2, respectively) are typically catalyzed by noble metals:^{1,2}



Numerous studies of methane oxidation over platinum-based catalysts have demonstrated that the catalytic activity in the low-temperature methane oxidation depends on the molar O₂/

CH₄ ratio. For instance, Burch and Loader³ showed that the methane conversion at 300–550 °C decreases in the series of molar ratios: O₂/CH₄ = 1:1 (fuel-rich) > O₂/CH₄ = 2:1 (stoichiometric) > O₂/CH₄ = 5:1 (fuel-lean). Furthermore, a sharp increase in the catalyst activity as the temperature rises was observed in the fuel-rich or stoichiometric but not in the

Received: July 4, 2014

Revised: February 26, 2015

Published: February 27, 2015

lean reaction mixtures. Similar results have been obtained by other researchers.^{4,5}

The observed changes in the catalytic activity can be attributed to the changes in platinum chemical state depending on the reaction mixture composition.⁶ An evident correlation between the O₂/CH₄ ratio and the surface composition of Pt/Al₂O₃ catalysis has been revealed recently by Skoglundh et al.⁷ By combining in situ time-resolved X-ray absorption spectroscopy and different transient experiments, the authors demonstrated that the surface O/Pt ratio changes, which in turn affects the methane oxidation rate. It was found that an oxygen-rich surface hinders the dissociative adsorption of methane, thus lowering the catalyst activity at oxygen excess. It is noteworthy that for Pt catalysts, neither a completely reduced nor a fully oxidized surface is optimal for methane oxidation. Instead, partially oxidized metal surfaces where the concentrations of adsorbed oxygen and methane are well balanced seem to be the most active.^{8,9}

The most explicit interpretation of the relationship between O₂/CH₄ ratio and the performance of Pt catalysts in CH₄ oxidation on the molecular level has been provided recently by Iglesia and co-workers.^{10,11} It has been shown that the O₂/CH₄ ratio determines the structure of the active sites on the rate-limiting stage of C–H bond activation. At a high O₂/CH₄ ratio, the C–H bond is activated over O^{*}–O^{*} pair sites via a homolytic hydrogen abstraction step. Over O^{*}–O^{*} sites, C–H bond activation barriers are high, and TOF is low because of the weak stabilization of the CH₃ fragments at transition states. In this regime, the rates depend linearly on the CH₄ pressure but are independent of the O₂ pressure. As the O₂/CH₄ ratio decreases, oxygen vacancies or exposed Pt atoms become available, and C–H bond activation proceeds over O^{*}–Pt site pairs via concerted oxidative addition and H-abstraction. In this regime, turnover rates increase significantly higher as a result of effective stabilization of the CH₃ fragments of the transition state by vacancies. The following decrease in the O₂/CH₄ ratio diminishes O^{*} coverages, and O₂ activation on bare Pt clusters becomes the sole kinetically relevant step. Under these conditions, the turnover rate becomes proportional to the O₂ pressures and independent of the CH₄ pressure.

On the other hand, several experimental observations remain unexplained. Table 1 summarizes some literature data on the

Table 1. Kinetic Parameters of the Methane Oxidation over Platinum Catalysts

catalyst	T, °C	O ₂ /CH ₄	order in		ref
			O ₂	CH ₄	
Pt/Al ₂ O ₃	300–500	2	0	0.9	12
Pt/Al ₂ O ₃ (porous)	500–559	0.7–2.2	0.75	1	13
Pt/Al ₂ O ₃ (nonporous)	500–559	0.5–3	1		14
Pt/Al ₂ O ₃ , Pt/TiO ₂ , Pt/ThO ₂	300–440	0.1–10	0	1	
Pt/Al ₂ O ₃	440	<2	0	-	15

influence of the reaction mixture components (methane or oxygen) on the process. The zero reaction order with respect to oxygen under the lean conditions and the first order under the rich conditions have been observed by some researchers,^{12,13} but other researchers have observed the zero-order reaction with respect to oxygen in both cases.^{14,15}

These data are in agreement with our earlier results on the effect of the O₂/CH₄ ratio on the activity of Pt/Al₂O₃ in

methane oxidation.¹⁶ Our data revealed the existence of two different steady-state regimes of Pt/Al₂O₃ catalyst performance in methane oxidation at identical O₂/CH₄ ratio: regimes of “low activity” and “high activity”. It was demonstrated that the low activity regime can be attained by decreasing the O₂/CH₄ ratio from 2:1 to 1.3:1. A further decrease in the O₂/CH₄ ratio results in a significant activity increase (high activity regime), and the catalyst retains high activity even after increasing the O₂/CH₄ ratio to 2.2:1. The appearance of such so-called “concentration hysteresis” allowed us to hypothesize that two different surface structures of Pt/Al₂O₃ catalyst can be attained depending on the catalyst “prehistory”. It was suggested that an “oxygen-rich” surface structure of low activity having a high O/Pt ratio is attained at a O₂/CH₄ ratio of ~2.5–2.2 and remains stable upon decreasing the O₂/CH₄ ratio to ~1. Upon decreasing the O₂/CH₄ below this limit, the Pt surface becomes depleted in oxygen, the O/Pt ratio decreases, and the catalyst is switched to the high activity regime. Thus, two regimes of high or low activity can be attained within the range of O₂/CH₄ ratio between 1.2–1.8.

To confirm our hypothesis that two different steady-state O/Pt surface structure of the catalyst are responsible for the observed concentration hysteresis, in this study, we performed a detailed kinetic investigation of methane oxidation in combination with an in situ X-ray absorption spectroscopy (XAS) study, which is a proven technique to probe the chemical state of Pt active species under reactive conditions.^{17–23} These data were complemented by a detailed study of the effect of adding CO and H₂ to the reaction mixture for the concentration hysteresis, as well as the effect of variation of CH₄ concentration.

2. MATERIALS AND METHODS

To prepare a catalyst for the study, the earlier developed procedure was used. It includes a wet impregnation of γ-alumina (SASOL TKA-432, surface area S_{BET} = 215 m²g⁻¹, granule size of 0.25–0.5 mm) with a platinum nitrate solution, followed by removal of excess solvent using a rotary evaporator. The amount of platinum supported on Al₂O₃ in the catalyst under study determined by atomic emission spectroscopy with inductively coupled plasma (Baird) was ~0.75 wt %. Finally, the sample was air-dried at 120 °C for 2 h and calcined in air at 400 °C for 4 h. According to transmission electron microscopy (TEM), X-ray absorption fine structure (XAFS), and X-ray photoelectron spectroscopy (XPS) data,²⁴ PtO₂ nanoparticles with a narrow particle size distribution are the initial form of the active component of thus-prepared catalysts.

Catalytic tests were carried out in a flow-circulation reactor BI-CATr at atmospheric pressure and constant temperature of 390 °C. Gases (O₂, N₂, CH₄) were cleaned from possible impurities using a BI-GASCleaner setup.²⁵ The construction of the BI-CATr setup has been described in detail elsewhere.^{26,27} This device complies with the principles of a recycle reactor.²⁸ In brief, this setup provides the gradientless mode, which allows measuring the activity of catalysts at a high accuracy because of the absence of temperature and concentration gradients inside the catalyst bed.²⁹ Gradientlessness of the setup has been tested experimentally. For this purpose, the activity of the catalyst has been measured using different catalyst loadings (0.5–20 g) but keeping the contact time constant (0.33 s). It has been found that such changes in the catalyst loading have not resulted in a change in the measured activity, which remains constant (0.0057 mL_{CH₄} g_{cat}⁻¹ s⁻¹).

The loaded catalyst (1.3 g) was heated in the inlet (initial) reaction mixture (IRM) containing oxygen (2.5 vol %), methane (1 vol %), and nitrogen. The hysteresis was studied by decreasing the O₂ concentration from 6.6 to 0.2 vol % in 0.2 vol % intervals followed by increasing the O₂ concentration in the same manner at a constant CH₄ concentration in the IRM. The flow rate of the reaction mixture was 240 mL/min. The multiplicity of the reaction mixture circulation throughout the catalyst bed was ~70, which was sufficient to free the catalyst bed of the concentration gradient (see above). The composition of the outlet (final) reaction mixture (ORM) was identical to the mixture composition over the operating catalyst. The ORM composition was determined after the stability of the stationary state was examined for an hour.

The influence of the CO, H₂ and H₂O concentrations in the inlet mixture on the hysteresis was studied. The concentrations of H₂, CO, and CH₄ in ORM were determined using a built-in high-speed chromatograph with thermocatalytic detector; the O₂ and CO₂ concentrations were measured by a Khromosib GKh1000 gas chromatograph. The concentration of water was calculated from the hydrogen mass balance. The conversion of methane was calculated on the basis of the methane consumption. Variations in the mixture volume during the reaction were negligible and, therefore, not taken into account.

The turnover frequency (TOF) value was determined using eq 3:

$$\text{TOF} = \frac{\frac{(C_{\text{CH}_4}^{\text{IRM}} - C_{\text{CH}_4}^{\text{ORM}}) \cdot U}{w_{\text{cat}}}}{D_M} \cdot \frac{M}{0.0075 \cdot 22400}, \text{ s}^{-1} \quad (3)$$

where *U* is the flow rate of the initial gas mixture (240 mL/min), C_{CH₄}^{IRM} and C_{CH₄}^{ORM} are the concentrations of methane in inlet and outlet reaction mixtures, *w_{cat}* is the weight of catalyst, D_M is the dispersion of Pt, *M* is the molecular mass (195.09 g mol⁻¹ for Pt), 0.0075 is the platinum loading, and 22400 is the factor for converting the milliliters of gas to the moles.

The number of the surface Pt atoms was calculated assuming that the metal particles are spherical and the dispersion D_M can be calculated from the surface average particle size, d_{vs} ($\sum V_i / \sum S_i$, nm) using eq 4:³⁰

$$D_M = \frac{6 \cdot V_m}{a_m \cdot d_{vs}} \quad (4)$$

where V_m is the atomic volume (nm³) and a_m is the average surface area occupied by one metal atom (nm²). In turn, V_m = (M × 10²¹) / (ρ × N_A) = 0.0151 nm³ and a_m = 1 × 10¹⁴ / σ = 0.08 nm². ρ is the density of Pt (21.45 g cm⁻³), N_A is the Avogadro's number (6.02 × 10²³ atoms mol⁻¹), and σ is the concentration of the metal atoms on the surface (1.25 × 10¹⁵ atoms cm⁻² for Pt).

Transmission electron microscopy (JEM-2010, Jeol Co.) was used to characterize the Pt particle size distribution on the support surface and to define the mean particle sizes for the synthesized catalyst. Prior to the TEM examination, the samples were ground and suspended in ethanol. A drop of the suspension was then mounted on a copper grid covered by a "holed" carbon film, and the solvent was evaporated. TEM measurements were performed at 200 kV and line-in-line resolution of 0.14 nm. Periodic images of the lattice structures on electron micrographs were analyzed using the digital Fourier transformation. The size distribution of the platinum crystallites was determined by measuring more than 500 particles.

The platinum dispersion was also determined by irreversible H₂ chemisorption. The original catalyst sample (0.1 g) was outgassed at 393 K in a He flow and then reduced in H₂ flow at 573 K prior to performing gas chemisorption experiments. The vacuum volumetric adsorption experiments were performed at 313 K in an automatic gas sorption analyzer Autosorb-1-C-MS/TCD (Quantachrome Instruments, Boynton Beach, FL, USA). The double isotherm method was used:³¹ the first isotherm obtained after 2 h of evacuation at 1 × 10⁻³ Torr and 573 K gave the total gas uptake, and the second isotherm obtained after 1 h of evacuation at 313 K gave the weakly adsorbed gas. The amount of irreversibly held H₂ was calculated as the difference between the amounts of the total and the weakly adsorbed H₂. The pressure range of the isotherms was 2–560 Torr, and an extrapolation to zero pressure was used as a measure of the gas uptake on the metal. A stoichiometric atomic ratio, H/Pt_s = 1 (Pt_s denotes a surface Pt atom), and the total Pt loading evaluated from the elemental analysis data were used to calculate platinum dispersion. The mean Pt crystallite sizes were determined from the H₂ chemisorption data using the site densities of 1.12 × 10¹⁹ sites/(m² of the metal).

The chemical state of Pt in the catalyst was investigated by XAS spectroscopy at the Structural Materials Science end-station of the National Research Center, Kurchatov Institute,³² using a reaction chamber designed for in situ measurements. Details of the reaction chamber design are given elsewhere.⁶ The Pt L₃-edge XAS spectra were measured in the transmission mode by means of two ionization chambers filled with appropriate mixtures of nitrogen and argon providing 20 and 80% absorption for I₀ and I_b, respectively. A Si(111) channel-cut monochromator was used. Platinum foil was used as a reference to calibrate the photon energy scale. For the measurements, the catalyst powder was pressed into a pellet with a diameter of 8 mm and a thickness of 1 mm and placed into the reaction chamber with a volume of ~5 l. The catalyst pellet prepared in such a way is characterized by a high permeability to reactive gases, which was tested in independent runs by successive reduction and reoxidation of the catalyst by H₂ and O₂.⁶

The methane oxidation over the catalyst was performed at 400 °C and 1 bar in a constant gas flow of 400 mL/min. The methane concentration was fixed at 1.0 vol % for all XAS measurements. The oxygen concentration was cycled from 0.5 to 4.0 vol % and back with intermediate points at 1.0, 1.5, 2.0, 2.5, and 3.0 vol % in both cases. Helium was used as an inert carrier. For each concentration point, the XAS spectra were measured consequently two times at 15 min intervals to check for chemical equilibration. The spectra were batch-processed using the IFEFFIT and LARCH software packages.^{33,34} Theoretical photoelectron amplitude and phase functions as calculated by the FEFF code were used in the fitting procedure.^{35,36} Experimental data were k²-weighted and fitted within the 2.0–12.0 Å⁻¹ range of photoelectron wavevectors. Coordination numbers and distances for two first-coordination shells, namely, Pt–O and Pt–Pt, were used as variable parameters. To reduce mutual correlations between fitable parameters, the amplitude reduction factor S₀² and zero-energy shift ΔE were fixed at 0.85 and 7.0 eV, respectively. Furthermore, the effective Debye–Waller factors, σ², for both coordination spheres were fixed at 0.01 Å² in analogy to data reported for similar catalysts.^{18,21}

3. RESULTS AND DISCUSSION

Catalyst Characterization. Figure 1a compares XANES spectra of the as-prepared catalyst and crystalline PtO_2

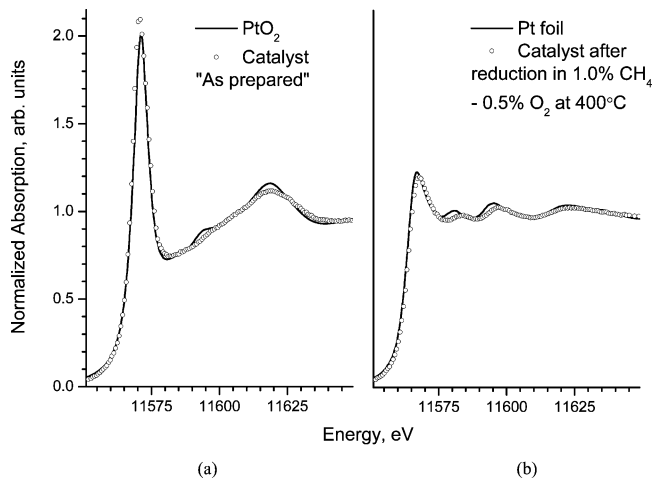


Figure 1. XANES spectra for the Pt catalyst as prepared (a) and after treatment with a mixture of CH_4 (1%) and O_2 (0.5%) at $400\text{ }^\circ\text{C}$ (b). The spectra were measured at room temperature in UHV and compared with the reference samples PtO_2 (a) and Pt foil (b).

reference. The white line intensity as well as the general shape of the Pt L_3 -edge XANES clearly indicate that the chemical state of platinum in the initial sample is close to Pt^{4+} . According to EXAFS (data not shown), the local environment of Pt atoms in the as-prepared catalyst includes at least three well resolved coordination spheres, namely, $\text{Pt}-\text{O}$ (5.3, 2.00 Å the first oxygen shell), $\text{Pt}\cdots\text{Pt}$ (5.6, 3.07 Å), and $\text{Pt}\cdots\text{O}$ (6.5, 3.66 Å the second oxygen shell) (the values in parentheses are best-fit coordination numbers and interatomic distances), which also correspond fairly well to crystallographic parameters of trigonal α -polymorph of PtO_2 .³⁷

As we mentioned above, the active component in such a catalyst should exhibit a high redox lability⁶ and can easily change its state, depending on the composition of the reaction medium. Indeed, the treatment in the $\text{CH}_4 + \text{O}_2$ reaction mixture (CH_4/O_2 ratio of 2) at $400\text{ }^\circ\text{C}$ reduces the Pt^{4+} ions to metallic platinum: the corresponding XANES spectrum measured *in situ* agrees completely with the spectrum of Pt metal (Figure 1b).

The TEM micrograph and the corresponding size distribution of platinum particles for the catalyst after its reduction are shown in Figure 2. The platinum particles visualized as dark spots (Figure 2a) are homogeneously dispersed on the alumina surface, the standard deviation from the mean particle diameter being $\sim 25\%$ (Figure 2b). The mean size of Pt particles and the corresponding value of dispersion (DM) calculated according to eq 4 are 2.1 nm and 53.6%, respectively. The latter value was used for the calculation of the TOF. It should be noted that the value of the platinum dispersion calculated from the H_2 chemisorption data is 48.8%, which corresponds to the mean particle size of 2.4 nm. Good agreement between TEM and chemisorption data suggests a nearly spherical shape of the Pt particles.

Catalytic Measurements. Typical hysteresis curves of the methane conversion as well as the yields of the products of the complete (CO_2 and H_2O , eq 1) and partial (CO and H_2 , eq 2) methane oxidation are shown in Figure 3. The data are

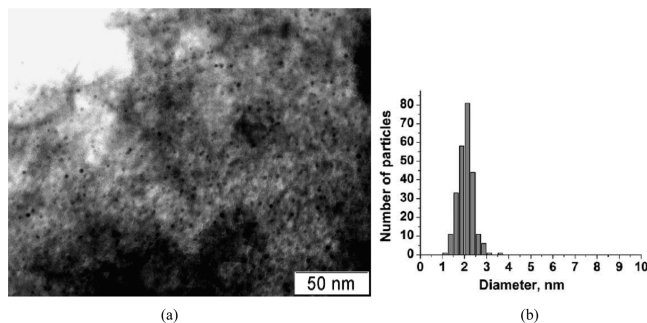


Figure 2. Transmission electron micrographs (a) and the particle size distribution (b) for the Pt catalyst after its reduction in H_2 at $400\text{ }^\circ\text{C}$. The interplanar spacing of $\sim 2.27\text{ \AA}$ on the high resolution images (not shown) corresponds to the crystal lattice of metallic platinum displaying the (111) lattice planes.

obtained as the O_2 concentration in the IRM is decreased (empty squares) and then increased (filled squares). The CH_4 concentration is kept constant at 1 vol %.

A low methane conversion (<12%) with CO_2 and H_2O as the only reaction products (Figure 3b, open symbols) is observed under the fuel-lean conditions ($\text{O}_2/\text{CH}_4 > 2:1$). A decrease in the O_2 concentration to 1.1 vol % does not lead to any significant changes in the product composition and reaction rate. This indicates zero-order kinetics with respect to oxygen. The overall reaction pattern is typical of a low activity regime of the catalyst. According to Iglesia et al., this is typical of CH_4 oxidation over oxygen-covered Pt surface having a high O/Pt ratio and activation of C–H bond over O^*-O^* pair sites.^{10,11} However, a further decrease in the O_2 concentration results in a noticeable activation of the catalyst. The methane conversion rose from $\sim 10\%$ to 35%. Simultaneous appearance of the partial oxidation products (H_2 , and some CO) is observed (Figure 3b, solid symbols). The following increase in the O_2 concentration is accompanied by an increase in the catalytic activity and a drop of the H_2 concentrations in the ORM. The maximum catalytic activity is reached at an O_2 concentration of 1.9 vol %. The overall reaction pattern is typical of switching the catalyst to the high activity regime and agrees with our previous data.

Using eq 4, methane conversions are recalculated to the values of TOF (see right axis y in Figure 3a). It is easy to see that the inactive state of the catalyst is characterized by a TOF value of $\sim 0.01\text{ s}^{-1}$ which can be increased to 0.063 s^{-1} after activation at rich conditions (compare TOF at O_2 concentration of 1.9 vol %). It should be noted that similar values of the TOF (0.005 s^{-1}) were reported for the dispersed phase of platinum in methane oxidation over $\text{Pt}/\text{Al}_2\text{O}_3$ catalysts at $335\text{ }^\circ\text{C}$ for 50 Torr of CH_4 and 110 Torr of O_2 in helium.³⁸

It is noteworthy that the catalyst behavior in the high activity regime is in a good agreement with the mechanism proposed by Iglesia et al. for CH_4 oxidation over an oxygen-depleted Pt surface, when the C–H bond is activated over O^*-Pt site pairs or even over bare Pt clusters, as indicated by the significant increase in the TOF and almost linear increase in TOF with O_2 concentration.^{10,11} However, the activity of the catalyst increases in parallel with the increase in O_2/CH_4 only to a ratio of ~ 2 , which corresponds to the stoichiometry for the reaction 1. A further increment of the O_2 content by 0.2 vol % leads to a sharp drop in the activity to the initial low level. The partial oxidation products disappeared completely upon achieving the initial low-active state of the catalyst. This change

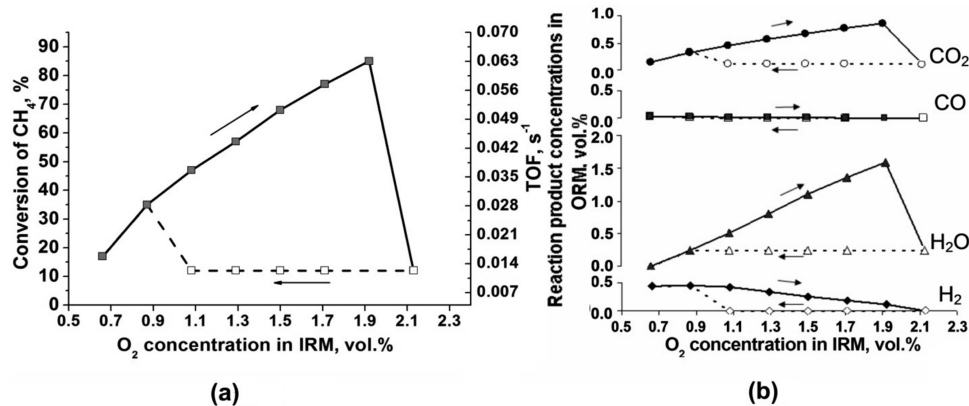


Figure 3. Methane conversion (a) and reaction product concentrations (b) at the decrease (open symbols, dashed lines) and subsequent increase (filled symbols, solid lines) in the O₂ concentration in the IRM. Conditions: 390 °C, 1 vol % CH₄.

in the catalyst performance suggests switching the catalyst to the low activity regime.

Both regimes of the catalytic system are stable and reproducible for the repeated cycles of varying of the O₂ concentration. Neither sintering nor coking of the catalyst is observed. It should be noted that switching the catalyst between the high activity and low activity regimes induced by changes in the feed composition takes less than 2–4 min.

In Situ XAS Measurements. To reveal a relationship between the oxidation state of Pt and its catalytic behavior in the regimes of high and low activity, the electronic structure of platinum particles in the catalyst and their transformations as a function of O₂/CH₄ ratio in the gas phase and the direction of its change were studied by in situ XAS.

Figure 4 shows a corresponding series of Pt-L₃ XANES spectra. One can see that the spectra are evidently grouped into

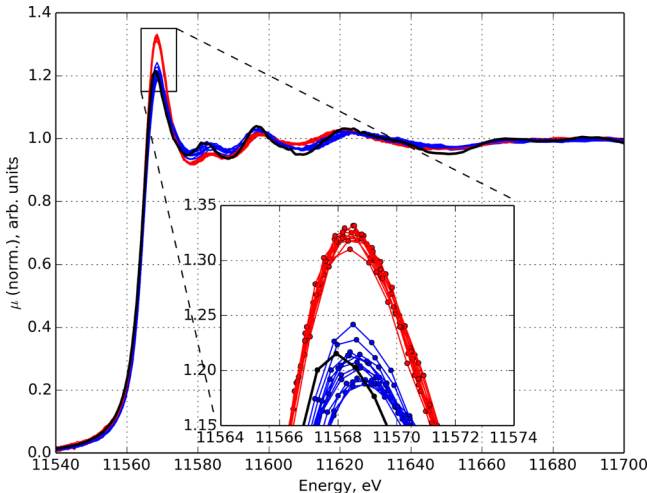


Figure 4. In situ Pt L₃-edge XANES measurements for the catalyst during methane oxidation for different oxygen ratios in the reaction mixture. Red curves, oxidized state of Pt; blue curves, reduced state of Pt; black curve, Pt foil reference.

two clearly nonequivalent electronic states of low (mostly reduced state, blue curves) and high (mostly oxidized state, red curves) white line intensities. It is noteworthy that there is no significant energy shift between positions of absorption maxima for the two states and only a minute shift to higher energies with respect to Pt foil reference (solid black curve in Figure 4).

These states are stable within specific concentration ranges of oxygen in the IRM, but these stability ranges depend on the direction of the oxygen concentration variation. The Pt switches from the mostly reduced to mostly oxidized state at 2.0–3.0 vol % of oxygen when increasing O₂ concentration and at 1.5–1.0 vol % upon decreasing. This results in an evident concentration hysteresis (Figure 5) resembling the hysteresis

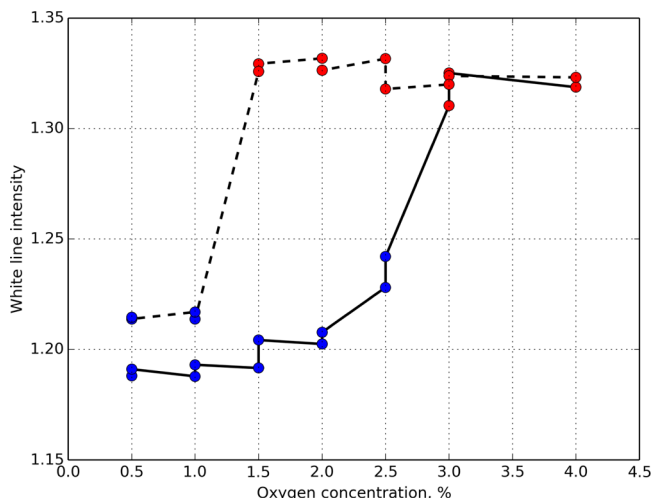


Figure 5. Intensity of the white line during in situ XANES measurements for the increase of oxygen concentration in the IRM (solid line) and subsequent decrease (dashed line).

loop observed in the catalytic experiments (compare Figure 3a and Figure 5). It is remarkable that the transition between two nonequivalent electronic states of platinum occurs at the same critical oxygen concentrations as in catalytic measurements shown in Figure 3.

It should be mentioned that a comprehensive description of the system points to a special behavior of a partially oxidized platinum state, which is identified by enhancing the intensity of the white line in Pt-L₃ XANES spectra at an O₂ concentration of 2.5% (Figure 5) to some intermediate level. This state appeared only upon an increase in the oxygen ratio. On one hand, this state can be responsible for the highest catalytic activity of the catalyst (Figure 3a, solid symbols on the upper part of the concentration hysteresis loop at O₂ concentration ~2%). This observation is in a good agreement with the data of Skoglundh et al.⁷ and Burch et al.,⁸ which indicates that the

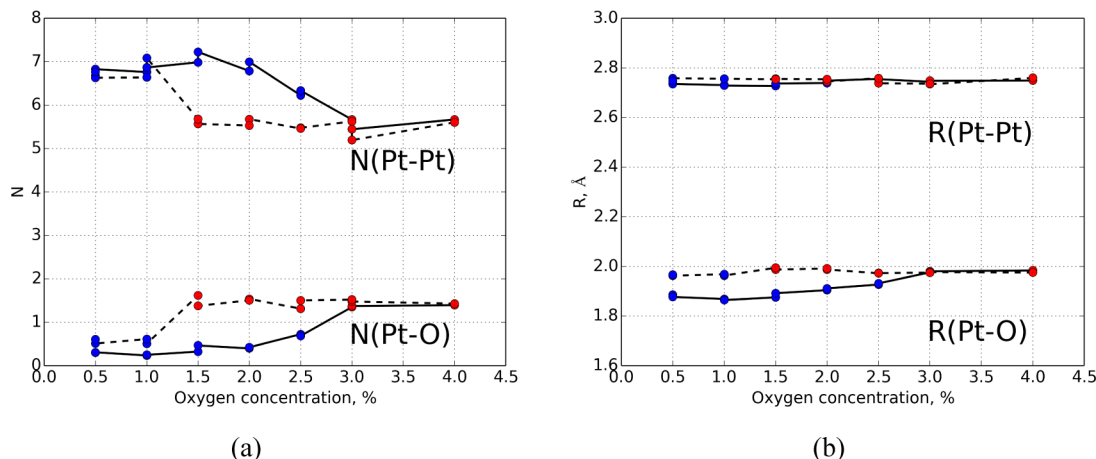


Figure 6. Coordination numbers (a) and interatomic distances (b) for the Pt–Pt and Pt–O shells obtained from EXAFS fits. Red curves, oxidized state of Pt; blue curves, reduced state of Pt. Solid line, increase in the oxygen concentration in the IRM; dashed line, subsequent decrease in the oxygen concentration in the IRM.

highest catalytic activity in methane oxidation can be attained over a partially oxidized platinum surface, rather than on the surface completely covered by oxygen or bare Pt.

On the other hand, small discrepancies in the O₂ concentrations that are characteristic of preliminary an increase in the white line intensity (~2.5%) and deactivation of the catalyst (~2.0%) can lead to another conclusion that even a first step of Pt oxidation reduces the catalyst activity in methane oxidation. It is evident that to clarify this observation, catalytic properties have to be measured in the same XAS experiment. Furthermore, observation of the “intermediate” oxidation state in XAFS, which is an ensemble-averaging technique, could be related to the nanoparticle size distribution. In particular, the smaller particles could be completely oxidized; the larger particles are only partially oxidized or even reduced; and when the ensemble is measured, an intermediate oxidation state might be apparent. Nevertheless, the conclusion about correlation between catalytic activity and electronic state of platinum is fully supported by analysis of EXAFS data presented in Figure 6 (more details and illustrations regarding EXAFS data processing can be found in the *Supporting Information*). Both the oxidized and reduced forms of platinum (red and blue dots, respectively) and the hysteresis loop are clearly seen in best-fit coordination numbers for Pt–O and Pt–Pt shells. Again, the switch between the two species of platinum occurs at the same critical oxygen concentrations as in the catalytic experiments shown in Figure 3 and XANES analysis in Figure 5.

The mostly reduced state of Pt in the catalyst is characterized by a Pt–O coordination number of ~0.5 and a Pt–Pt coordination number of 7. According to theoretical estimates,¹⁷ values around 7 for Pt–Pt coordination numbers in reduced platinum samples should correspond to a mean particle size of about 1.5 nm at room temperature, which is rather close to the size actually determined for the catalyst by TEM (2.1 nm). The mostly oxidized form of the catalyst is characterized by a slightly increased Pt–O coordination number (~1.5) and correspondingly decreased Pt–Pt coordination number (5.5). No significant change in the Pt–O and Pt–Pt interatomic distances is observed along the concentration hysteresis loop. Similar behavior was earlier observed in an *in situ* XAS study of methanol oxidation over Pt nanoparticles (0.7 nm) supported on γ -Al₂O₃.³⁹ For example, treatment of the reduced Pt/ γ -

Al₂O₃ sample in a CH₃OH/O₂ mixture at 50 °C changes the Pt–Pt coordination number from 7 to 5.5, keeping the Pt–Pt interatomic distance around a value of 2.756 ± 0.004 Å.³⁹ Thus, the evident correlation between our XAS and catalytic data strongly suggests that switching the catalyst between the low activity regime and the high activity regime, causing the concentration hysteresis, stems from changing the electronic state of the Pt particles. In turn, the changes in Pt electronic state are attributable to changes in the O/Pt surface ratio caused by a variation of the oxygen concentration in the reaction mixture.

Influence of the Reaction Mixture Composition and the Temperature on the Hysteresis. Our experimental data indicate also that the sharp increase in the catalytic activity and reduction of platinum is accompanied by the appearance of H₂ (and CO in some experiments⁶) in the gas phase (Figure 1). These products of the partial oxidation of methane may cause a reduction of platinum. However, the reaction of the partial oxidation does not start until the catalyst switches to the high activity regime. What are the reasons and consequences in such situation? Therefore, it is of interest to understand the influence of the products and reactants on the activity, selectivity, and conditions of the transition between the low and high active states of the supported platinum.

Effect of H₂ and CO Addition. A series of experiments were carried out by hydrogen addition to the initial mixture at a constant concentration of methane (1 vol %). Typical results on the impact of adding 0.6% H₂ are shown in Figure 7. The only effect of the hydrogen addition is a shift in the hysteresis loop along the *x* axis toward a higher O₂ concentration by ~0.3% of oxygen. At the same time, neither the hysteresis width nor the catalyst performance changes.

The effect of the hydrogen concentration on the hysteresis loop was studied by variation of the hydrogen concentration from 0 to 3 vol %. The results are displayed in Figure 8a as the relationship between the concentration of added H₂ and the O₂ concentration causing deactivation (filled squares) and activation (empty triangles), that is, switching between the low activity and high activity regimes. The linear approximation of these data with a proportionality coefficient of ~0.5 indicates that the shift of the hysteresis loop corresponds to the stoichiometry of the oxidation of hydrogen with oxygen (H₂ + (1/2)O₂ → H₂O). This observation suggests that additional

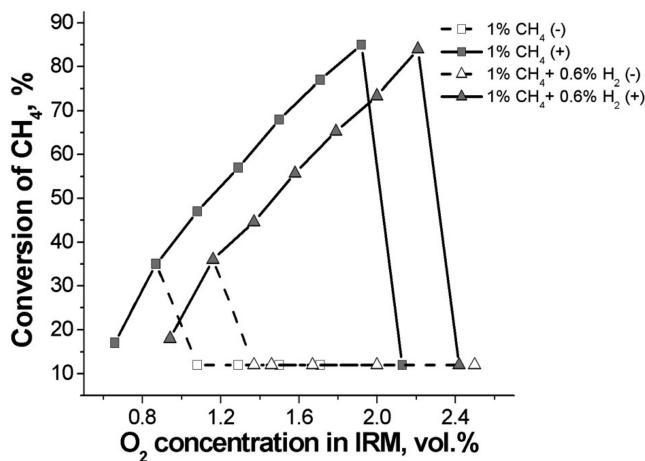


Figure 7. Shift of the hysteresis loop at the addition of 0.6 vol % H₂ to the initial mixture. Dotted line and solid line correspond to the CH₄ conversion at the decrease and subsequent increase in the O₂ concentration, respectively. Conditions: 390 °C, 1 vol % CH₄.

hydrogen is not involved in the initiation of the hysteresis but mostly consumed in the oxidation, thus decreasing the effective oxygen concentration.

Analogous experiments with CO added to the reaction mixture gave similar results: addition of CO had no impact on the hysteresis width, while the loop was shifted along the hysteresis loop along the axis of the O₂ concentration by the distance corresponding to the stoichiometry of CO oxidation (Figure 8b). All of these data suggest that the catalyst switch to the high activity regime is triggered when the oxygen partial pressure (actually, the oxygen chemical potential) decreases below a certain limit, and H₂ or CO act as “oxygen scavengers” by consuming stoichiometric amounts of oxygen.

Effect of CH₄ Concentration. The effect of the CH₄ concentration in the IRM on the hysteresis loop was studied by variation of CH₄ concentration from 1 to 3 vol %, in other words, by adding an extra amount of methane to the initial concentration of 1 vol %. The results are shown in Figure 9a. There is an evident difference between the impact of H₂ or CO on the hysteresis loop and the CH₄ concentration effect. Unlike H₂ or CO, additional CH₄ not only shifts the hysteresis loop

toward a higher oxygen concentration but also leads to an increase in the “O₂ concentration width” of the hysteresis.

Analysis of the relationship between the CH₄ concentration and the O₂ concentration of switching between the low activity and high activity regimes is shown in Figure 9b. Clearly, the slopes of activation and deactivation relations are different, which reflects the change in the hysteresis loop width. The coefficients of linear correlations between CH₄ and O₂ concentration for activation and deactivation events are given in Figure 9b. Tentatively, these data can be rationalized as follows: Switching from the low activity regime to the high activity regime occurs as the CH₄/O₂ ratio in the reaction mixture becomes close to the stoichiometry of partial CH₄ oxidation (2). On the other hand, switching from the high activity regime back to low activity regime (catalyst deactivation) takes place as CH₄/O₂ ratio approaches the stoichiometry of the total methane oxidation and the reaction mixture tends to be enriched in O₂.

On the basis of the data presented in Figure 9, two important conclusions on the catalyst performance in low activity regime and high activity regime can be made:

- (1) High activity regime (filled symbols in Figure 9a). One can see that the catalyst activity increases with increasing CH₄ concentration, as indicated by higher turnover rates at fixed O₂ concentrations. The increase in the oxygen concentration also improves the reaction rate at all CH₄ concentrations studied. The observed dependences are in good agreement with the kinetics of CH₄ oxidation over a partially oxygen-depleted surface of Pt when the C–H bond is activated over O^{*}–Pt site pairs, as was demonstrated by Iglesia et al.^{10,11} In addition, clear dependence of the reaction rate on the CH₄ concentration allows us to exclude activation of the C–H bond over a bare platinum surface because such activation suggests independence of the CH₄ partial pressure, in accordance with the Iglesia model.^{10,11}
- (2) Low activity regime (open symbols in Figure 9a). As was mentioned above, in the low activity regime, the turnover rate is independent of the O₂ concentration, in agreement with the CH₄ oxidation over an “oxygen-saturated” Pt surface and activation of the C–H bond over O^{*}–O^{*} pair sites.^{10,11} On the other hand, the

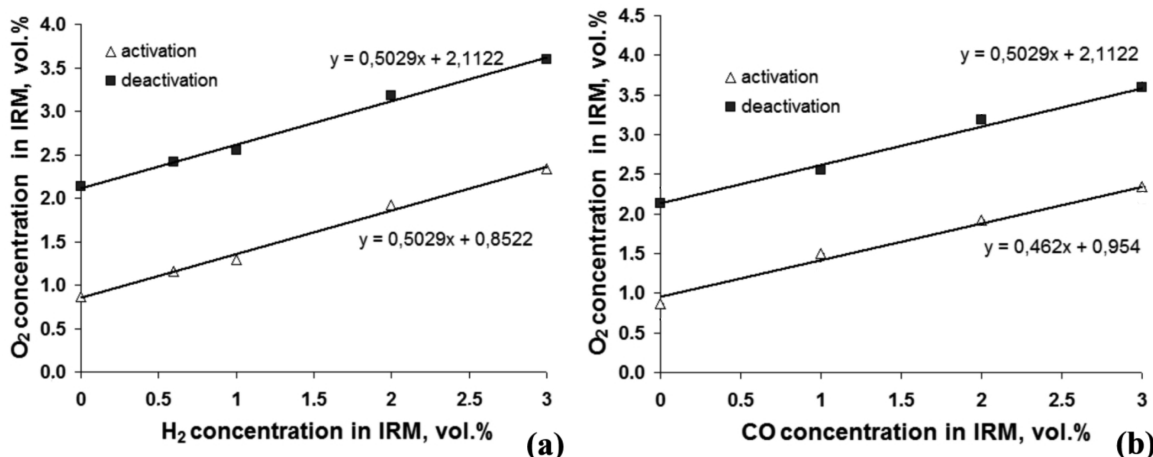


Figure 8. O₂ concentration corresponding to activation and deactivation of the catalyst as a function of the H₂ (a) and CO (b) concentrations in the initial mixture. Conditions: 390 °C, 1 vol % CH₄.

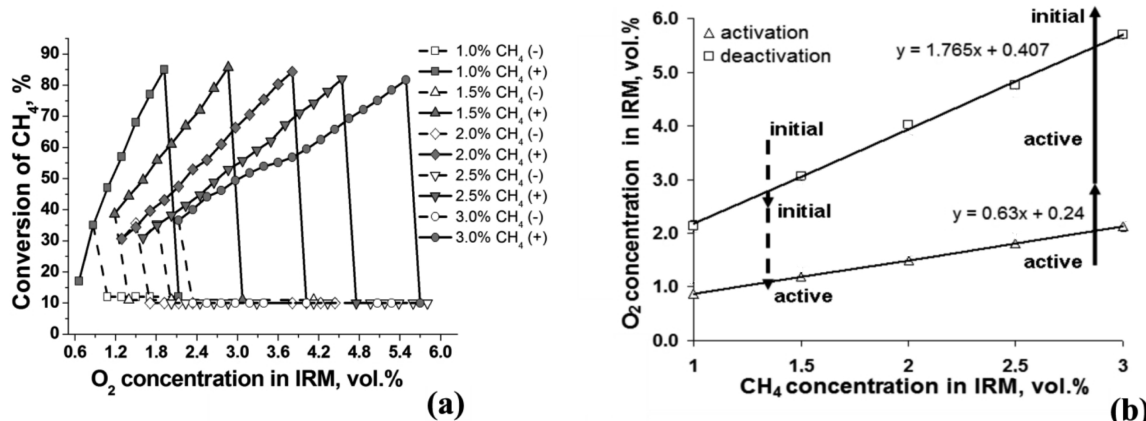


Figure 9. (a) Conversion of CH_4 at the decrease (dotted line) and the subsequent increase (solid line) in the O_2 concentration. The methane concentration in the initial mixture varies from 1 to 3 vol %. Conditions: $390\text{ }^\circ\text{C}$. (b) The O_2 concentration corresponding to the activation and deactivation of the catalyst versus the CH_4 concentration in the IRM. The arrows indicate the activation of the system with a decrease in the O_2 concentration (dashed arrow) and the reverse deactivation with a further increase in the O_2 concentration (solid arrow).

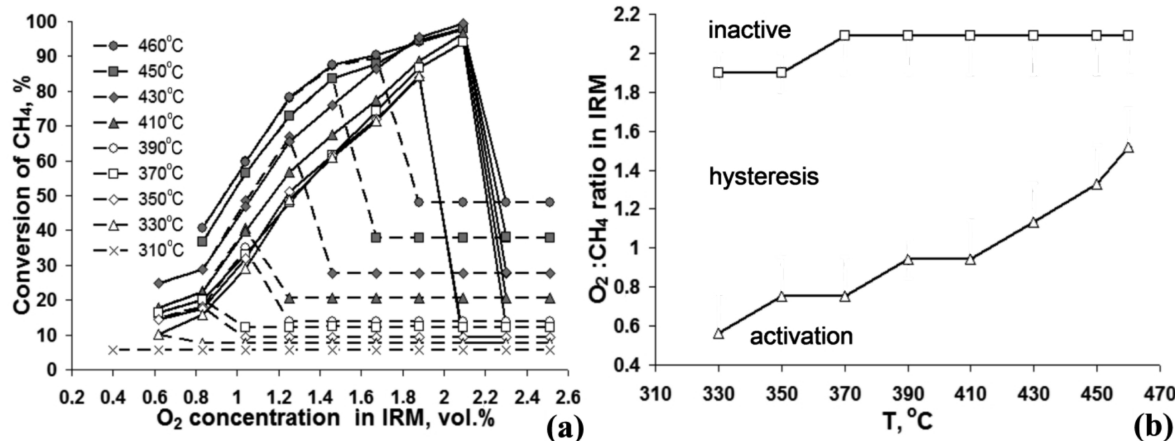


Figure 10. (a) The impact of temperature on the hysteresis. (b) The effect of the temperature on the oxygen content causing the activation and deactivation of the catalyst. CH_4 concentration = 1 vol %.

turnover rate shows low sensitivity to the CH_4 concentration, as well, which is in contrast with the Iglesia model.

This discrepancy deserves additional discussion. Analysis of our XANES and EXAFS data along with the observed reaction kinetics allows us to suggest a formation of a surface oxide-like structure over the surface of Pt particles in the low activity regime. Formation of a surface oxide rather than an adsorbed oxygen is expected to cause a marked change in the structure of the active sites and kinetically relevant step. For Pt catalysts, such an effect is demonstrated in several reactions: oxidation of CH_4 ,^{8,9} CO ,^{40,41} and C_3H_8 .^{42,43} Our EXAFS and XANES data provide additional evidence for such a hypothesis. Thus, XANES data reveal a strong increase in the white line intensity upon switching the catalyst to the low activity regime. In addition, EXAFS data show the decrease in the Pt–Pt coordination numbers from ~ 7 to ~ 5.5 after the transition of the catalyst to the low activity regime, which can be interpreted as a formation of a smaller metal core covered by a two-dimensional layer of surface Pt oxide. Formation of the bulk PtO_x oxides seems to be excluded by the consistency of the absorption peak maximum at various CH_4/O_2 ratios (Figure 3), as opposed to the higher energy shift of Pt L_3 XANES spectra when metallic platinum transforms to PtO , Pt_3O_4 , or PtO_2 .²³

Of course, such speculations should be considered with caution, because DFT calculations demonstrated that oxygen adsorption on $\text{Pt}(111)$ increases the number of unoccupied d states, thus increasing the white line intensity.⁷

It is noteworthy that the results obtained by Iglesia¹⁰ exclude the formation of oxide-like structures, unlike our results. However, we should take into account that the experiments in ref 10 were performed at 873 K ($600\text{ }^\circ\text{C}$), whereas in our experiments, the temperature was significantly lower. Thermodynamic data⁴⁴ for Pt, Pt_3O_4 , and PtO_2 point to increasing stability of the oxide structures as the temperature decreases. Thus, the lower temperature in our experiments may favor formation of oxide-like structures on the Pt surface in the low activity regime, which, in turn, causes specific kinetics and the appearance of the hysteresis phenomenon.

To confirm the above speculations, the catalyst performance upon variation of O_2 concentration is compared for various temperatures in the range of 310 – $460\text{ }^\circ\text{C}$, and the data are summarized in Figure 10. It is evident that at $310\text{ }^\circ\text{C}$, the catalyst exhibits the performance typical for the low activity regime without an apparent hysteresis loop. The hysteresis loop appears as the reaction temperature rises to $330\text{ }^\circ\text{C}$, indicating that a certain temperature threshold is required for switching the catalyst between the low activity regime and the high

activity regime. Indeed, as the reaction temperature rises, the hysteresis loop becomes narrower and tends to disappear at temperatures above 500 °C.

This observation is in line with our argument for the formation of surface oxide in the low activity regime and its destabilization above 500 °C as a result of the exothermic nature of Pt oxide formation. Destabilization of Pt oxide prevents switching the catalyst to the low activity regime, which results in the disappearance of the hysteresis phenomenon. Within the 330–500 °C interval, switching the catalyst between the low and high activity regimes is triggered by changing the oxygen partial pressure (oxygen chemical potential) resembling phase transition $\text{Pt}^0 \leftrightarrow \text{Pt oxide}$.

It should be noted that the literature data on Pt oxide formation in the course of oxidation are contradictory. For example, Pt oxide formation has been ruled out by Iglesia on the basis of kinetics measurements and XRD data.^{10,45} On the other hand, Pt oxide formation has been detected by Olsson and Fridell using a surface sensitive XPS technique.⁴⁶

4. CONCLUSIONS

Oxidation of methane over a Pt/ $\gamma\text{-Al}_2\text{O}_3$ catalyst was studied at 310–460 °C as a function of oxygen concentration. It has been found that two distinct regimes of the catalyst performance can be attained at identical compositions of the reaction mixture: a low activity regime and a high activity regime. Switching between the regimes depends on the O₂ concentration and the direction of its change: an incremental decrease in O₂ concentration from 2.5% (lean conditions) to approximately 1% (rich conditions) results in catalyst activation and its switching to the high activity regime. The catalyst remains active upon a further incremental increase in O₂ concentration until reaching O₂/CH₄ ~ 2, when switching to the low activity regime takes place. Such responses of the catalyst activity to gas composition changes result in the appearance of a pronounced concentration hysteresis. In turn, the changes in Pt electronic state are attributable to changes in O/Pt surface ratio or formation/decomposition of a two-dimensional layer of surface Pt oxide triggered by variation of the oxygen concentration in the reaction mixture.

The evident correlation between XAS and catalytic data strongly suggests that the switching of the catalyst between the low and high activity regimes, causing the concentration hysteresis, stems from changing the electronic state of the Pt particles. In the low activity regime, the Pt-L₃ white line intensity increases, indicating an increased number of unoccupied d states and a decreased electron density on the Pt species. On the other hand, upon switching the catalyst to the high activity regime, the electron density on the Pt species increases, as evidenced by a lowering of the white line intensity. The changes in the Pt electronic state are attributable to changes in the O/Pt surface ratio caused by the variation of the oxygen concentration in the reaction mixture.

The addition of highly reactive CO or H₂ to the reaction mixture shifts the hysteresis loop toward a higher oxygen concentration because of consuming oxygen in H₂ or CO oxidation, thus decreasing the effective oxygen concentration. In contrast to this, the increase in the methane concentration widens the hysteresis window, presumably because of the different stoichiometry of the CH₄ oxidation upon catalyst activation (when partial oxidation of CH₄ prevails) and deactivation (when total oxidation of CH₄ predominates).

Thus, the catalyst performance can be improved significantly by changing the prehistory of the sample without varying the reaction temperature, contact time, or catalyst composition. As our catalytic results demonstrate, the methane conversion can be increased by several times by activation of the catalyst at rich conditions. However, treatment of the catalyst in lean reaction mixtures deactivates the catalyst. Thereby, studies of the concentration hysteresis may open a way to control the activity and selectivity of Pt catalysts for the oxidation process.

■ ASSOCIATED CONTENT

S Supporting Information

The following file is available free of charge on the ACS Publications website at DOI: 10.1021/cs501964z.

Normalized EXAFS functions and Fourier transforms for the whole series of in situ measurements as well as representative results of fits ([PDF](#))

■ AUTHOR INFORMATION

Corresponding Author

*Phone: +7 (383) 330 67 71. Fax: +7 (383) 330 83 56. E-mail: vib@catalysis.ru.

Notes

The authors declare no competing financial interest.

■ ACKNOWLEDGMENTS

This work was supported by a Grant of the President of the Russian Federation (MK-5340.2014.3) and RFBR (project Nos. 12-03-01104 and 13-03-01003). XANES measurements were performed at the User Facility “Kurchatov Center for Synchrotron Radiation and Nanotechnology” supported in part via the Russian Federal Contract No. 16.552.11.7055.

■ REFERENCES

- (1) Gelin, P.; Primet, M. *Appl. Catal., B* **2002**, *39*, 1–37.
- (2) Choudhary, T. V.; Banerjee, S.; Choudhary, V. R. *Appl. Catal., A* **2002**, *234*, 1–23.
- (3) Burch, R.; Loader, P. K. *Appl. Catal., B* **1994**, *5*, 149–164.
- (4) Lyubovsky, M.; Smith, L. L.; Castaldi, M.; Karim, H.; Nentwick, B.; Etemad, S.; LaPierre, R.; Pfefferle, W. C. *Catal. Today* **2003**, *83*, 71–84.
- (5) Oh, S. H.; Mitchell, P. J.; Siewertt, R. M. *J. Catal.* **1991**, *132*, 287–301.
- (6) Veligzhanin, A. A.; Zubavichus, Y. V.; Chernyshov, A. A.; Trigub, A. L.; Khlebnikov, A. S.; Nizovskii, A. I.; Khudorozhkov, A. K.; Beck, I. E.; Bukhtiyarov, V. I. *J. Struct. Chem.* **2010**, *51*, S20–S27.
- (7) Becker, E.; Carlsson, P.-A.; Gronbeck, H.; Skoglund, M. *J. Catal.* **2007**, *252*, 11–17.
- (8) Burch, R.; Loader, P.; Urbano, F. *Catal. Today* **1996**, *27*, 243–248.
- (9) Carlsson, P.-A.; Fridell, E.; Skoglundh, M. *Catal. Lett.* **2007**, *115*, 1–7.
- (10) Chin, Y. H.; Buda, C.; Neurock, M.; Iglesia, E. *J. Am. Chem. Soc.* **2011**, *133*, 15958–15878.
- (11) Garcia-Dieguez, M.; Chin, Y. H.; Iglesia, E. *J. Catal.* **2012**, *285*, 260–272.
- (12) Niwa, M.; Awano, K.; Murakami, Y. *Appl. Catal., A* **1983**, *7*, 317–325.
- (13) Trimm, D. L.; Lam, C.-V. *Chem. Eng. Sci.* **1980**, *35*, 1405–1413.
- (14) Cullis, C. F.; Willatt, B. M. *J. Catal.* **1983**, *83*, 267–285.
- (15) Firth, J. G.; Holland, H. B. *Trans. Farad. Soc.* **1969**, *65*, 1121–1127.
- (16) Pakharukov, I. Yu.; Bekk, I. E.; Matrosova, M. M.; Bukhtiyarov, V. I.; Parmon, V. N. *Dokl. Phys. Chem.* **2011**, *439*, 131–134.

- (17) Frenkel, A. I.; Hills, C. W.; Nuzzo, R. G. *J. Phys. Chem. B* **2001**, *105*, 12689–12703.
- (18) Sanchez, S. I.; Menard, L. D.; Bram, A.; Kang, J. H.; Small, M. W.; Nuzzo, R. G.; Frenkel, A. I. *J. Am. Chem. Soc.* **2009**, *131*, 7040–7054.
- (19) Cuenya, B. R.; Croy, J. R.; Mostafa, S.; Behafarid, F.; Li, L.; Zhang, Z.; Yang, J. C.; Wang, Q.; Frenkel, A. I. *J. Am. Chem. Soc.* **2010**, *132*, 8747–8756.
- (20) Mostafa, S.; Behafarid, F.; Croy, J. R.; Ono, L. K.; Li, L.; Yang, J. C.; Frenkel, A. I.; Cuenya, B. R. *J. Am. Chem. Soc.* **2010**, *132*, 15714–15719.
- (21) Cuenya, B. R.; Frenkel, A. I.; Mostafa, S.; Behafarid, F.; Croy, J. R.; Ono, L. K.; Wang, Q. *Phys. Rev. B* **2010**, *82*, 155450–1–8.
- (22) Friebel, D.; Miller, D. J.; O’Grady, C. P.; Anniyev, T.; Bargar, J.; Bergmann, U.; Ogasawara, H.; Wikfeldt, K. T.; Pettersson, L. G. M.; Nilsson, A. *Phys. Chem. Chem. Phys.* **2011**, *13*, 262–266.
- (23) Merte, L. R.; Behafarid, F.; Miller, D. J.; Friebel, D.; Cho, S.; Mbuga, F.; Sokaras, D.; Alonso-Mori, R.; Weng, T.-C.; Nordlund, D.; Nilsson, A.; Cuenya, B. R. *ACS Catal.* **2012**, *2*, 2371–2376.
- (24) Beck, I. E.; Bukhtiyorov, V. I.; Pakharukov, I. Yu.; Zaikovsky, V. I.; Kriventsov, V. V.; Parmon, V. N. *J. Catal.* **2009**, *268*, 60–67.
- (25) Bobrov, N. N.; Leonov, A. S.; Belov, A. N.; Demidov, M. B.; Titov, V. N.; Vanin, E. A.; Lipishanov, P. P. *Catal. Ind.* **2005**, *2*, 50–58.
- (26) Pakharukov, I. Yu.; Bobrov, N. N.; Parmon, V. N. *Catal. Ind.* **2009**, *1*, 38–42.
- (27) Pakharukov, I. Yu.; Bobrov, N. N.; Parmon, V. N. *Catal. Ind.* **2009**, *2*, 95–101.
- (28) Berty, J. M. *Experiments in Catalytic Reaction Engineering*; Elsevier: Amsterdam, New York, 1999; p 268; 978-0-444-82823-1.
- (29) Bobrov, N. N.; Parmon, V. N. *Principles and Methods for Accelerated Catalyst Design and Testing*; Derouane, E., Parmon, V., Lemos, F., Ribeiro, R., Eds.; Kluwer. Publishers: Dordrecht, 2002; p 197.
- (30) Anderson, J. R. *Structure of Metallic Catalysts*; Academic Press: London, 1975; p 296.
- (31) Sinfelt, J. H.; Carter, J. L.; Yates, D. J. *C. J. Catal.* **1972**, *24*, 283–296.
- (32) Chernyshov, A. A.; Veligzhanin, A. A.; Zubavichus, Y. V. *Phys. Res. A: Nucl. Instrum. Methods* **2009**, *603*, 95–98.
- (33) Ravel, B.; Newville, M. *J. Synchrotron Radiat.* **2005**, *12*, 537–541.
- (34) Newville, M. *J. Phys.: Conf. Ser.* **2013**, *430*, 012007–1–7.
- (35) Rehr, J. J.; Zabinsky, S. I.; Ankudinov, A.; Albers, R. C. *Physica B* **1995**, *208/209*, 23–26.
- (36) Zabinsky, S. I.; Rehr, J. J.; Ankudinov, A. *Phys. Rev. B* **1995**, *52*, 2995–3009.
- (37) Hoekstra, H. R.; Siegel, S.; Gallagher, F. X. *Adv. Chem.* **1971**, *98*, 39–53.
- (38) Hicks, R. F.; Qi, Y.; Young, M. L.; Lee, R. G. *J. Catal.* **1990**, *122*, 280–294.
- (39) Merte, L. R.; Ahmadi, M.; Behafarid, F.; Ono, L. K.; Lira, E.; Matos, J.; Li, L.; Yang, J. A.; Cuenya, B. R. *ACS Catal.* **2013**, *3*, 1460–1468.
- (40) Carlsson, P.-A.; Österlund, L.; Thormählen, P.; Palmqvist, A.; Fridell, E.; Jansson, J.; Skoglundh, M. *J. Catal.* **2004**, *226*, 422–434.
- (41) Ackermann, M.; Pedersen, T.; Hendriksen, B.; Robach, O.; Bobaru, S.; Popa, I.; Quiros, C.; Kim, H.; Hammer, B.; Ferrer, S.; Frenken, J. W. M. *Phys. Rev. Lett.* **2005**, *95*, 255505–1–4.
- (42) Carlsson, P.-A.; Mollner, S.; Arnby, K.; Skoglundh, M. *Chem. Eng. Sci.* **2004**, *59*, 4313–4323.
- (43) Yoshida, H.; Yasawa, Y.; Hattori, T. *Catal. Today* **2003**, *87*, 19–28.
- (44) Muller, O.; Roy, R. J. *Less-Common Metals* **1968**, *16*, 129–146.
- (45) Weiss, B. M.; Iglesia, E. *J. Phys. Chem. C* **2009**, *113*, 13331–13340.
- (46) Olsson, L.; Fridell, E. *J. Catal.* **2002**, *210*, 340–353.